

## Risk Assessment of Uniform Corrosion and Localized Corrosion of Alloy 22

A. Passarelli<sup>1</sup>, D. Dunn<sup>2</sup>, O. Pensado<sup>2</sup>, T. Bloomer<sup>3</sup>, and T. Ahn<sup>3</sup>

<sup>1</sup>U.S. Nuclear Regulatory Commission, Region I, King of Prussia, PA 19406-1415

<sup>2</sup>Center for Nuclear Waste Regulatory Analyses, San Antonio, TX 78238-5166

<sup>3</sup>U.S. Nuclear Regulatory Commission, Washington, D.C. 20555-0001

### ABSTRACT

The risk associated with the performance of Alloy 22 waste package (WP) in the potential repository for high-level nuclear waste at Yucca Mountain was assessed using the NRC's Total-system Performance Assessment (TPA) Code. The high temperature (above 100° C) deliquescence relative humidity from mixed salt deposits on the WP surface was evaluated by lowering the critical relative humidity ( $RH_{critical}$ ) for aqueous corrosion to (35 - 60) pct. For the base case values of the critical potential for localized corrosion, the estimated dose increased from 0.05 to 1 mrem/year in 10,000 years by altering  $RH_{critical}$ . For the modified case the estimated dose increased to 3.8 mrem/year at 10,000 years without lowering  $RH_{critical}$ . With the addition of nitrate as an inhibitor, the estimated dose decreased to 0.03 mrem/year at 10,000 years. Giving credit to the remaining surface area of the WP after failure by localized corrosion reduces the estimated dose from 4 mrem/year to 0.4 mrem/year. Anodic sulphur segregation at the interface of metal and passive film and subsequent spalling of passive film may enhance uniform corrosion. The cyclic process of fast active corrosion upon sulfur segregation followed by slow passive corrosion upon repassivation is unlikely to reduce significantly the WP lifetime.

## INTRODUCTION

An important attribute of the high-level waste (HLW) disposal program in the U.S. is the estimated long lifetime of waste packages (WPs). It has been proposed that the WP be constructed of Alloy 22, a Ni-Cr-Mo (Ni-22Cr-13Mo-3W-4Fe) alloy known to be resistant to localized corrosion in chloride containing environments. The WP performance in the potential Yucca Mountain (YM) repository has been assessed with mathematical models of various WP corrosion modes in conjunction with various models representing the behaviors of geology, hydrology and other components of engineered barrier system (EBS). The NRC's Total-system Performance Assessment (TPA) Code (i.e., Code) utilizes several mathematical models, incorporating geological, hydrological and chemical effects, to evaluate risk to the public from the WP failure <sup>[1]</sup>. The Code allows to perform sensitivity analyses to estimate how changes in the environment of the inside of YM could affect the corrosion behavior of Alloy 22 WP, over a time period of 10,000 years. The results are expressed in terms of 'risk' (the likelihood times consequences of the radionuclide release). The WP failure is defined as occurring when the thickness of the outer container (approximately 2 cm) of the WP is penetrated by a corrosion process. This may occur as a result of localized corrosion or accelerated uniform corrosion through the rolled and machined cylindrical shell portion of the container.

After the ventilation period and repository closure, WP surface temperatures above 100°C are expected for several hundred years. During this period, with the drip shields (DSs) diverting the dripping groundwater, mineral dusts will possibly deposit in the adsorbed thin film of water on the hot WP surface <sup>[2]</sup>. In the absence of the DS protection, the groundwater will directly drip on the hot WP surface provided that the drift wall temperature is below boiling. These two processes may result in mixed salt deposits on the WP surface, which in turn may concentrate dripping groundwater, decrease the deliquescence relative humidity (RH), and increasing the

boiling point of the solution <sup>[2,3]</sup>. Because the deliquescence relative humidity is dependent on the composition of the mixed salts, the deliquescence points of different compositions of groundwater over a broad range of RH values were input to the Code. In the absence of inhibitors to the WP corrosion, two sets of chloride chemistry were considered as (i) unmodified base case and (ii) modified case, that included different sets of data and data regressions for mill annealed and welded Alloy 22 under the same aqueous conditions. In these two cases, failure of the WP by a single through wall penetration was conservatively assumed to provide no protection for the WP contents. In order to calculate the effect of partial credit for WP after failure, the Code was programmed to measure radionuclide releases from the container with varied amounts of corroded area by localized corrosion as pitting as well as stress corrosion cracking. Crediting the remaining surface area following the corrosion process was an effective way to accomplish meaningful comparisons of results and interpreting associated risk. The presence of nitrate, which is known to inhibit crevice and pitting corrosion in chloride containing environments, was simulated in the Code by modifying parameters used to determine the initiation of localized corrosion.

The corrosion potential was calculated in the Code on the basis of a kinetic expression for the cathodic reduction of oxygen and water and the passive current density for the anodic dissolution of Alloy 22. Empirically derived equations calculated the dependence of critical potentials for localized corrosion on environmental parameters. The repassivation potential as the critical potential for localized corrosion depends on chloride concentration and temperature and is given by

$$E_{\text{crit}} = E_{\text{crit}}^{\circ}(T) + B(T)\log[\text{Cl}^-] \quad (1)$$

Where  $E_{crit}^{\circ}(T)$  and  $B(T)$  are linear functions of temperature. The unmodified base case parameters considered a limited set of data to define the repassivation potential as a function of chloride concentration and temperature. Modified case parameters corresponded to refining the empirical correlation to define the repassivation potential.

To complement results from the sensitivity studies using the Code, a separate mathematical model was constructed to assess the effect of enhanced uniform corrosion. A simple calculation was conducted to estimate how a fast (active or non-passive) and slow (passive) cyclic corrosion process, possibly due to anodic sulfur segregation in the alloy, could affect the WP lifetime. The premise of this assessment is that anodic sulfur segregation would possibly occur at the interface of the metal and the passive film causing the passive oxide layer to spall off [4]. Enhanced or accelerated uniform corrosion would then occur in these regions for a period of time before the passive layer can reform. This process could periodically repeat depending on the passive corrosion rate of Alloy 22 and processes that promote segregation of sulfur.

## METHODS

Critical relative humidity,  $RH_{critical}$ , is input to the Code that determines the relative humidity (RH) necessary to have a sufficiently thick water film on the WP that will support corrosion reactions. For most metals, the value of the  $RH_{critical}$  is similar and usually in the range of 60 to 70 percent (pct). Deliquescence of dust or salt deposits from evaporated seepage waters may reduce the  $RH_{critical}$ . The value of the  $RH_{critical}$  was altered to simulate deliquescence of mixed salts and evaluate their effects on the overall repository performance. As the Code processes a set of

given environmental RH values expected during the disposal time, if the RH is higher than the  $RH_{critical}$  for aqueous corrosion, the WP container will start degrading by aqueous corrosion. The corrosion mode (uniform or localized) is determined using a comparison of the critical potential for crevice corrosion to the corrosion potential and is described in subsequent paragraphs. The base case value of  $RH_{critical}$  (60-65) pct was altered to (35-60) pct, to reflect the scope of different mixed salts and their deliquescence points <sup>[5]</sup>. The aqueous chemistry for the WP surface from mixed salt deposits is likely dominated by alkaline brines of  $Na^+/K^+$  containing  $Cl^-$  and  $NO_3^-$  anions, and near neutral  $Mg^{2+}/Ca^{2+}$  chloride-dominated brines as a minor brines <sup>[6]</sup>. The deliquescence point of mixed salts is lower than the deliquescence point of binary mixtures <sup>[7]</sup>. At relatively high temperatures localized corrosion could take place because the repassivation potential decreases significantly with increasing temperature. Although localized corrosion data of Alloy 22 or C-4, which is a similar alloy in corrosion resistance to Alloy 22, are available in mixed brines, some uncertainties exist especially at temperatures greater than 100 °C in the mixed salt brines. Therefore, the sensitivity study is conducted assuming localized corrosion would occur.

The dependence of the critical potential on chloride concentration and temperature is given in Equations (1), (2), and (3).

$$E_{crit}^{\circ}(T) = A_1 + A_2 T \quad (2)$$

$$B(T) = B_1 + B_2 T \quad (3)$$

The terms  $E_{crit}^{\circ}(T)$  and  $B(T)$  are linear functions of temperature.  $A_1$  and  $A_2$  are parameters in the intercept term, and  $B_1$  and  $B_2$  are parameters in the slope term. These relationships are based on experimental data for mill annealed Alloy 22 in pure chloride solutions. Below Table (1) provides the unmodified base case parameters and the more recently modified parameter

inputs to the Code. Figure (1) is the repassivation potential as a function of temperature for mill annealed Alloy 22 in pure chloride solutions.

Table (1) Repassivation Potential Parameters for the Unmodified Base Case and the Modified Case

Parameter (units)	A <sub>1</sub> (mV <sub>SHE</sub> )	A <sub>2</sub> (mV/°C)	B <sub>1</sub> (mV)	B <sub>2</sub> (mV/°C)
Base	2006.0	-15.2	-590.7	4.3
Modified	1541.0	-13.1	-362.7	2.3

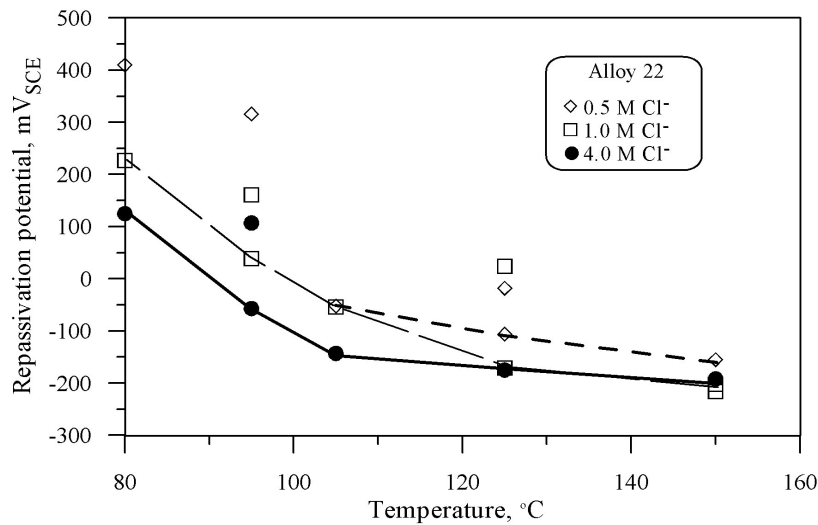


Figure (1) Repassivation Potentials as a Function of Temperature for Mill Annealed Alloy 22 in Pure Chloride Solutions [7]

The chloride concentration was systematically varied. - The concentrations of other anions found in J-13 well water were maintained at low values such that the influence of sulfates, bicarbonates, nitrate, and fluoride was likely minimal. It is known from experimental evidence as shown in Figure (2) below that above a nitrate to chloride concentration ratio of 0.2 (which

would be about 0.1 M nitrate) inhibits localized corrosion for both welded and mill annealed Alloy 22. Sufficient concentrations of nitrate to chloride that inhibit localized corrosion were simulated using a constant value of the repassivation potential with a value of 250 mV vs. SCE (500 mV vs. SHE).

For the unmodified base case and the modified case, no credit was given to the remaining surface area following penetration of the WP by localized corrosion. To be more realistic, another factor was changed in the Code to study the effect of localized corrosion on the radionuclide release through perforations expected from localized corrosion, giving credit to the remaining surface area. As the Code does not have this factor in conjunction with the WP corrosion, it was simulated by controlling the exposed surface area of spent nuclear fuels with Cladding Correction Factor in the Code. This Cladding Correction Factor simulates the actual exposed surface area of spent nuclear fuels to the aqueous environment. To credit the surface area that would remain in the WP after pitting (regardless of crevice corrosion) approximate determination of pit size and density was needed. These were determined from the literature to be only in certain small areas to be the size between  $10^{-4}$  to  $10^{-1}$  cm, and the density between  $10^{-1}$  to  $10^2$  per  $\text{cm}^2$  of the WP surface area for various alloys and environmental conditions [8]. An example of the density and the size of pits from generic potentiodynamic tests are shown in Figure (3). The resulting fraction of the exposed surface area is in the range of  $10^{-9}$  to 1 by combining pit size and pit density, which is the parameter changed in the Code. Similarly, the release from stress corrosion cracks were also tested using the literature data [9]. The fraction of the exposed surface area from stress corrosion cracking,  $\sim 1.1 \times 10^{-4}$ , was encapsulated in the pitting fraction. This value was obtained from about 25 cracks of the size,  $1.02 \text{ cm}^2$ , with respect to WP surface area of  $2.3 \times 10^5 \text{ cm}^2$ .

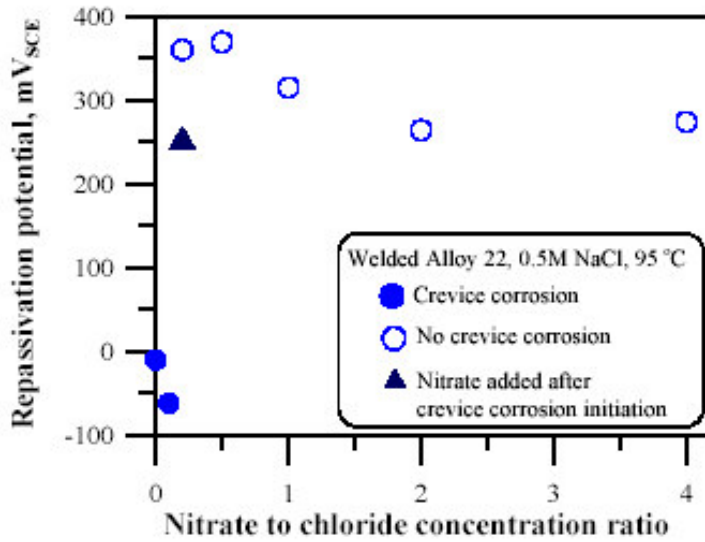


Figure (2) Repassivation Potentials as a Function of Nitrate to Chloride Ratio of Welded Alloy 22 in 0.5M NaCl at 95 °C

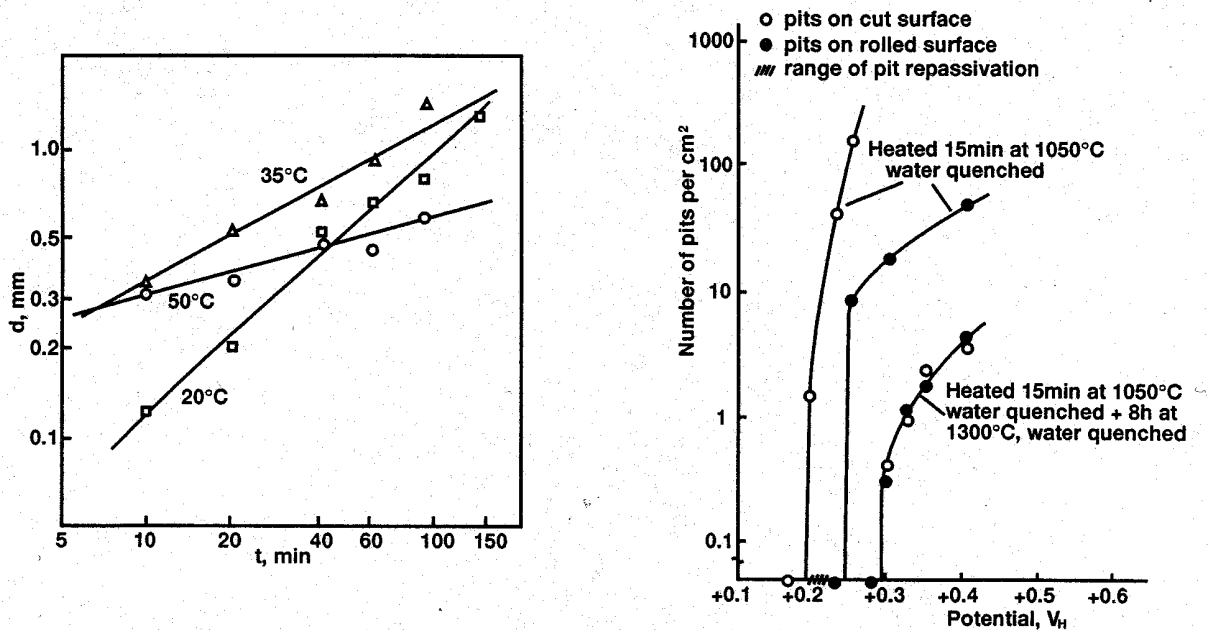


Figure (3) Examples of Size and Distribution of Pits. Pit diameter vs. Time for 18Cr-12Ni-2Mo-Ti Stainless Steel in 0.1N H<sub>2</sub>SO<sub>4</sub> + 0.1N NaCl. Normal Pit Size Observed is in the Range of μm to mm<sup>[10]</sup>, and Pit density is for 304 Stainless Steel after Potentiostatic Polarization in 1M NaCl Solution<sup>[10]</sup>. “d” is Pit Diameter and “t” is Time. (Reprinted with Permission)



A calculation was performed to assess the effect of slow and fast cyclic process of uniform corrosion on the WP lifetime. A transient enhanced dissolution process could occur due, for example, to anodic sulfur segregation at the metal-oxide interface or film spallation. Jones<sup>[4]</sup> estimated that it would take approximately 180 years to form a mono-layer of sulphur at the metal-oxide interface in nickel-based alloys containing 100 appm sulphur, assuming a uniform corrosion rate of  $10^{-2} \mu\text{m/year}$ <sup>[4]</sup>. Enhancement of the corrosion rate depends on the persistence of a sulfur compound (such as nickel sulfide) in the metal film. It is unlikely that sulfur compounds could persist in Ni-Cr-Mo alloys. The presence of molybdenum counteracts the effect of sulfur possibly by the formation of soluble molybdenum-sulfur compounds<sup>[11]</sup>. Thus, sulfur is removed from the system at a rate proportional to the rate of molybdenum dissolution. On the other hand, chromium has a low affinity for sulfur, but high affinity for oxygen; thus, the formation of chromium oxide competes with the formation of sulfur compounds. Given the abundance of oxygen and the presence of molybdenum in Alloy 22, the stability of sulfur compounds in the film for extended periods is unlikely. A protective oxide film should eventually form after the sporadic occurrence of enhanced dissolution rates due to anodic sulfur segregation, if this process were to occur. It has been argued that film spalling could also occur due to the accumulation of metal vacancies at the metal-film interface resulting from the passive dissolution process<sup>[12]</sup>. Also, a protective oxide must re-form after a transient state of free dissolution.

The rate of slow corrosion ( $CR_p$ ) times the period of time for slow corrosion ( $Ct_p$ ), plus the rate of fast corrosion ( $CR_f$ ) times the period of time for fast corrosion ( $Ct_f$ ), equals the amount corroded (i.e., penetration depth).

$$\text{Penetration Depth} = \sum [CR_p * Ct_p + CR_f * Ct_f] \quad (4)$$

The fast corrosion rate was estimated from the current transient prior to repassivation after immersing bare metal coupons. This current transient also gives the times for fast corrosion. An example of the anodic current transient and total charge transfer as a function of time is shown in Figure (4) for Alloy 22 at 100 mV vs. SCE in 0.028 M Chloride solution at 95 C<sup>[7]</sup>. The slow corrosion rate is obtained from potentiostatic tests<sup>[7]</sup> and the slow corrosion time is obtained by extrapolating the sulphur segregation time postulated by Jones<sup>[4]</sup> to the slow corrosion rate. Fast corrosion rates and times were varied to study the effect on the WP lifetime.

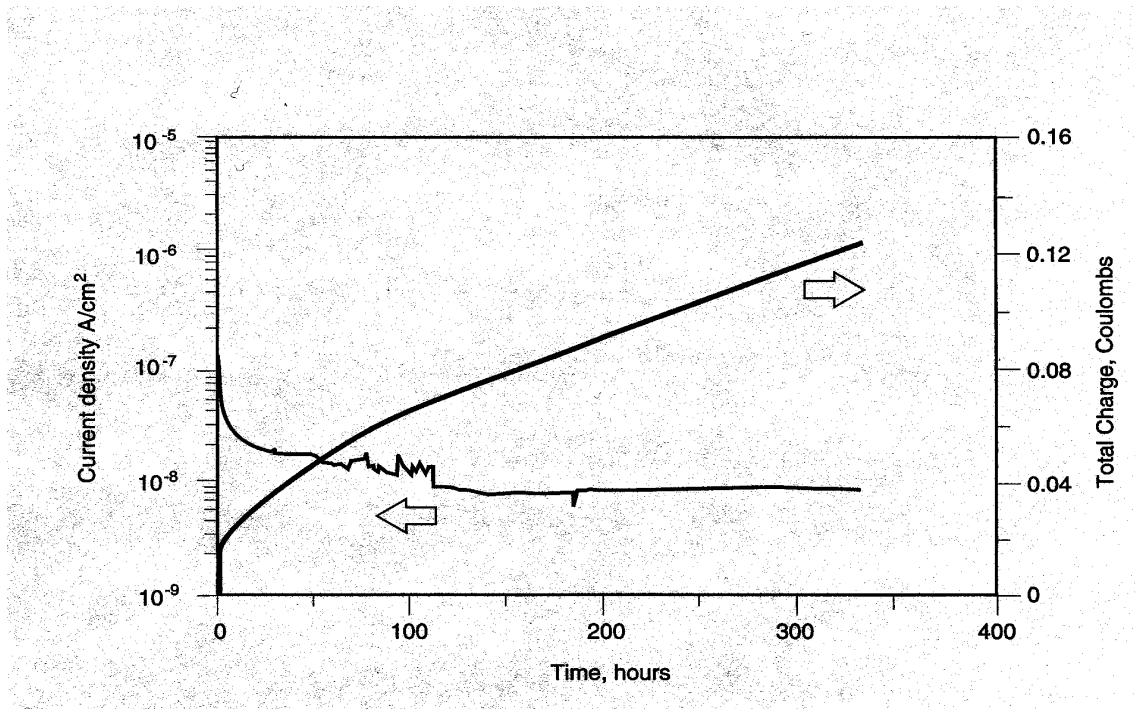


Figure (4) Anodic Current Density and Total Charge as a Function of time Measured on Alloy 22 at 100 mV<sub>sce</sub> in 0.028 M Chloride Solution at 95 °C [7]

### ANALYSIS RESULTS AND DISCUSSION

The Code was run in the base case with a changed range of  $RH_{critical}$  for localized corrosion to incorporate the high temperature deliquescence RH of mixed salts. With the greater range of  $RH_{critical}$  the Code calculated an estimated dose of about 1 mrem/year by 10,000 years as shown in Figure (5). This is in contrast to the unmodified base case (i.e.  $RH_{critical} = (60-65)$  pct) which resulted in an estimated dose of 0.05 mrem/year. Using the modified case of the repassivation potential with the base case range of  $RH_{critical}$  values, an estimated dose of 3.8 mrem/yr was obtained at 10,000 years as shown in Figure (6).

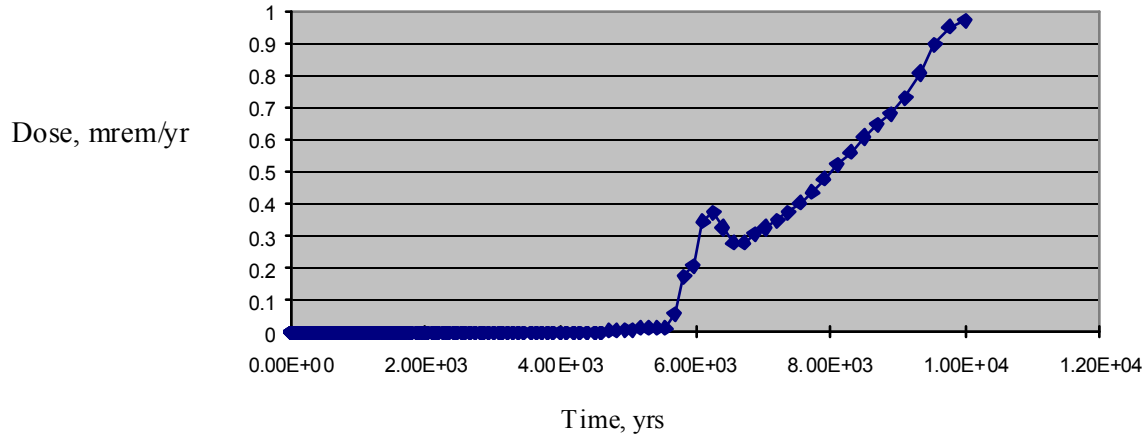


Figure (5) Estimated Dose in the Base Case of Repassivation Potential with a Changed Range of  $RH_{critical}$ , (35 – 60) pct, to Incorporate the High Temperature Deliquescence RH of Mixed Salts

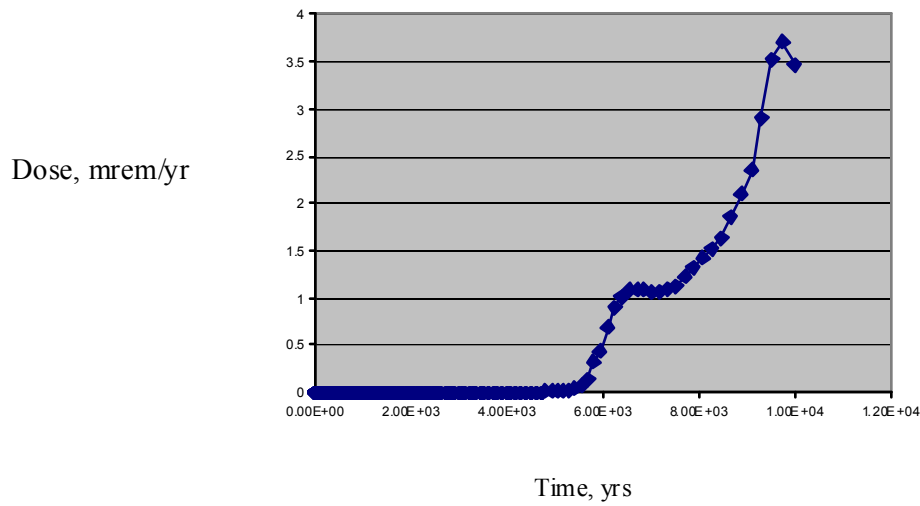


Figure (6) Estimated Dose in the Modified Case of Repassivation Potential with No Changed Range of  $RH_{critical}$

When the WP container is breached, it is assumed that all the spent nuclear fuel assemblies in each WP will be exposed for dissolution as bare matrices of spent nuclear fuels and no credit is given to the remaining surface area following localized corrosion. In the Code, Cladding Correction Factor can be used to assign the remaining surface area. Because the low deliquescence RH is mainly derived from near neutral  $Mg^{2+}/Ca^{2+}$  chloride-dominated brines that are not considered dominant brines, a low but finite probability exists for the aqueous corrosion at high temperatures (120–160 °C) [2]. Therefore, it is expected that the current exercise with modified distribution of  $RH_{critical}$  would not be very unrealistic, although it is likely to be still aggressive.

The calculation resulted in an estimated dose of 0.03 mrem/year at 10,000 years with nitrates as an inhibitor as shown in Figure (7). The DS was not included to add conservatism. Incorporating the nitrate effect substantially changed the estimated dose using the modified repassivation potential. It is expected that other anions such as carbonates, bicarbonate, and to a lesser extent sulfate may also enhance the passivity. Silica may deposit as a protective barrier too.

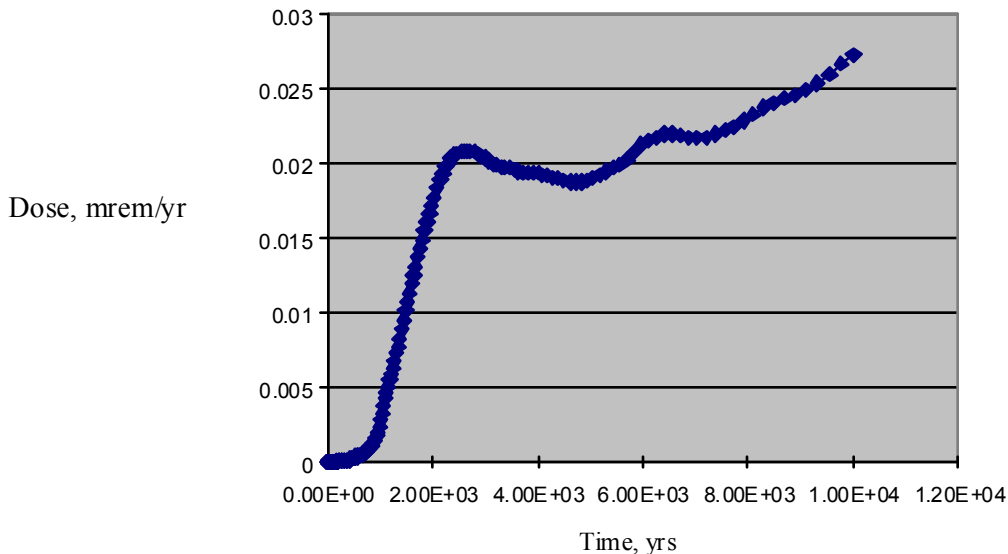


Figure (7) Estimated Dose with Nitrates as an Inhibitor

The data that were used to calculate the nitrate effect using the modified repassivation potentials results from an experiment where the chloride concentration was held constant and the concentration of nitrates was varied for welded and mill annealed Alloy 22 materials. Above a nitrate to chloride concentration ratio of 0.2 (which would be about 0.1 M nitrate), localized corrosion was inhibited. The repassivation potential increases with nitrate concentration and reaches a value in the range of 250 mV vs. SCE (500 mV vs. SHE) prior to complete inhibition of localized corrosion. If the constancy of the repassivation potential from the experiment with nitrates is applied to this equation, the repassivation potential for mill annealed Alloy 22 at 95° C is estimated to be 296 mV vs. SCE. Although the corrosion potential can increase as time elapses, it is unlikely for localized corrosion to occur with a nitrate to chloride concentration ratio above 0.2. Modification of the repassivation potential parameters was performed to explore the effect of a wide range of temperature and the nitrate to chloride ratio. Incorporating the nitrate effect substantially changed the estimated dose using the modified repassivation potential equation.

To be more realistic by giving credit in the radionuclide release to the unaffected remaining container surface area after localized corrosion, Cladding Correction Factor was changed in the Code. The results are shown in Figure (8). The curve on the top is the run with the modified case of repassivation potential without credit to the remaining surface area. The curve on the bottom has the added fraction of surface area exposed from localized corrosion as  $10^{-9}$  to 1. This range of the fraction of surface area exposed was obtained from the square of pit size times the pit density. The data on the pit size and pit density were given in the previous section as  $(10^{-4} - 10^{-1})$  cm and  $(10^{-1} - 10^2)/\text{cm}^2$ . With the surface area credit, the maximum estimated dose decreases from about 4 mrem/year to about 0.4 mrem/year. Similar results were obtained for release from stress corrosion cracks. Uncertainties exist for the fraction of surface area exposed from localized corrosion. The values of the fraction of surface area exposed,  $10^{-9}$  to 1,

are postulated for the sensitivity studies. Experimental values for Alloy 22 in the YM environment are not available. However, most of similar data in literature were obtained under applied potentials. Under open circuit conditions below pitting potential (or breakdown potential) and above the repassivation potential, continuous increase of pit generation and eventually total metal consumption is unlikely to occur. While under applied potentials the generation and propagation of pits are accelerated, pits could be stifled under open-circuit free conditions, as potential drops and throwing power decreases. Evidence in some alloys indicates stifling of localized corrosion under the open circuit conditions <sup>[13,14]</sup>. In addition, the aqueous corrosion conditions in thin film of water are generally known to be less conservative. For example, the separation of anode and cathode and reduced aqueous conductivity may promote stifling of localized corrosion too. Additionally, pitting corrosion is expected to occur in the crevice. If the crevice area is limited, the fraction of surface area exposed would be limited even though pits are generated continuously. The potential stifling of pits and the limited crevice area appear to limit the fraction of surface area exposed.

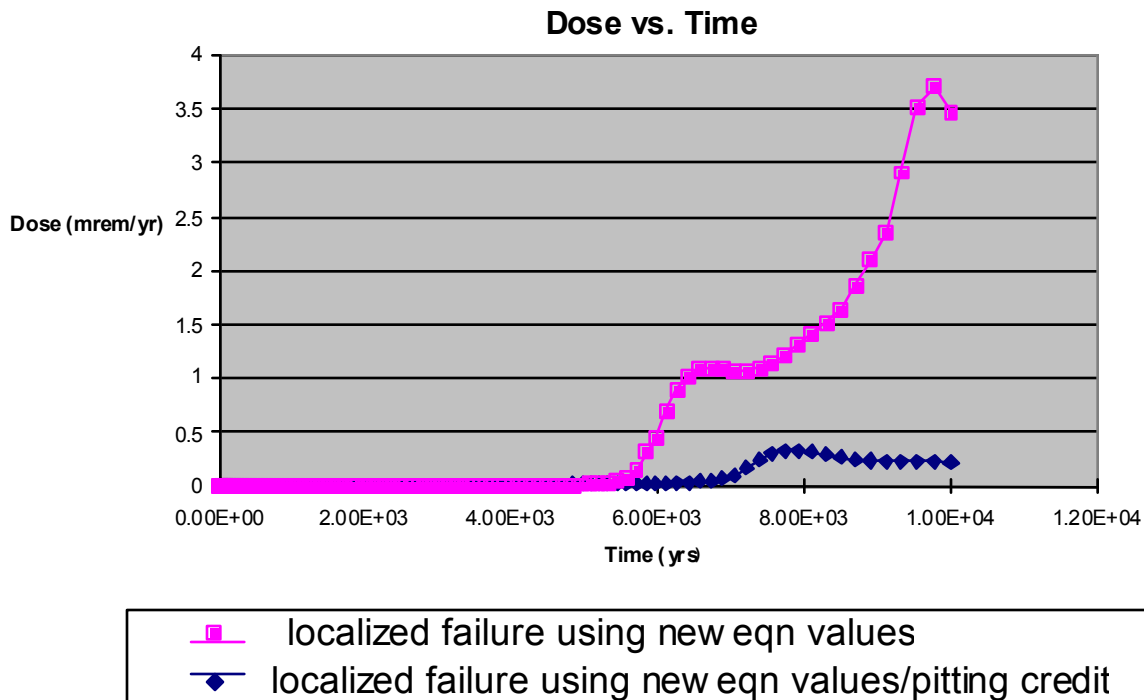


Figure (8) Estimated Dose by Giving Credit in the Radionuclide Release to the Remaining Container Surface Area after Localized Corrosion in Comparison with No Credit

For the mathematical calculation involving cyclic processes of slow and fast corrosion, the WP will be breached when the combined processes of slow and fast corrosion eventually corrodes through the WP. On the graph shown in Figure (9), lifetime is on the y-axis. Fast corrosion time on a log scale is the x-axis. The points are at the different fast corrosion times and the different curves represent different fast corrosion rates. The fast corrosion rates were varied from  $10^{-4}$  to  $10^{-2}$  cm/year; the fast corrosion times were varied from  $1.19 \times 10^{-4}$  to 1.19 year. The reference fast corrosion rate was obtained from the current transient of Figure (4). The transient total charge before the steady state was divided by the transient time to get the reference fast corrosion rate. It was  $\sim 1.04 \times 10^{-4}$  cm/year. A perturbation to  $10^{-2}$  cm/year is made to include uniform corrosion rates where the passive film is not stable. Whereas the current transient curve of Figure (4) was obtained from the tests with air-exposed coupons, the cyclic process



due to the oxide spallation would expose more pristine surface. This will in turn increase the transient current. Nevertheless,  $10^{-2}$  cm/year is an unrealistically extreme value to see the functional behavior of the penetration depth of Equation (4). A reference fast corrosion time was also obtained from the current transient curve of Figure (4). The transient time before the steady state was 0.0119 years. A perturbation was made from this reference value to see the sensitivity of the potential effects of segregated sulfur or corrosion potential variation.

The slow corrosion rate is an average value,  $10^{-4}$  cm/year, currently used in TPA <sup>[1]</sup>. The slow corrosion time is 1.8 years. From Jones' postulate <sup>[4]</sup>, it would take about 180 years at corrosion rate,  $10^{-6}$  cm/year, to form a mono-layer of sulphur at the interface of the film and bare nickel-based alloys containing 100 appm sulphur. Therefore, it would take 1.8 years at  $10^{-4}$  cm/year. However in a separate presentation, Jones discussed that an alloy with 100 appm of sulfur corroding at  $10^{-4}$  cm/year will accumulate a monolayer of sulfur on the surface in 500 years <sup>[15]</sup>. The severe condition of 180 years at  $10^{-6}$  cm/year was adopted here for the purpose of the sensitivity study.

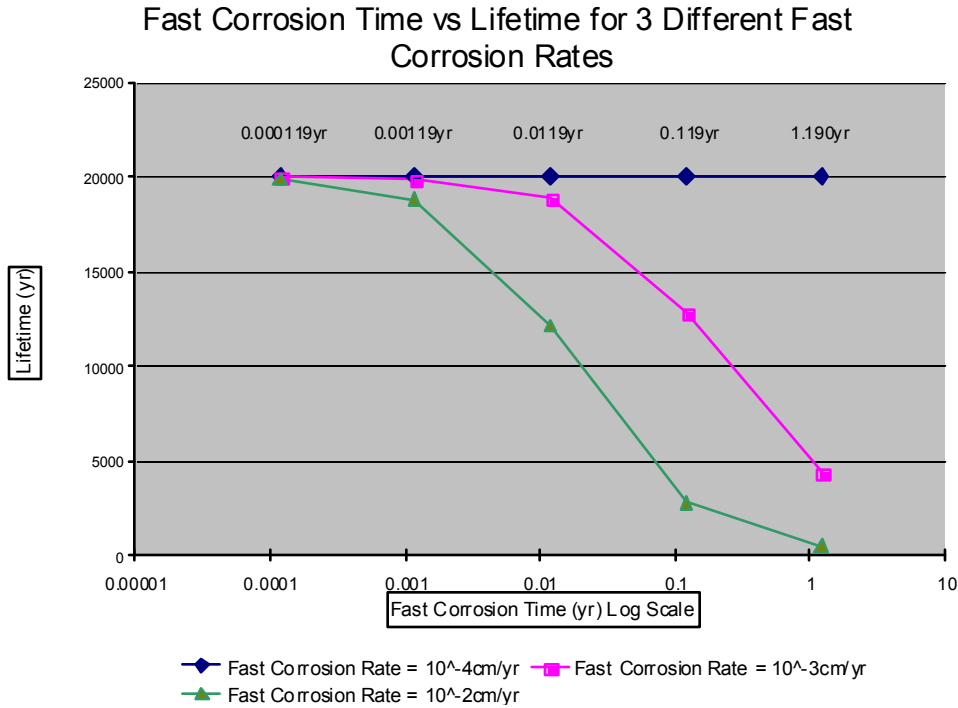


Figure (9) Waste Package Lifetime Involving Cyclic Processes of Slow and Fast Corrosion from Sulfur Segregation

With a small time period of fast corrosion, the variation of the corrosion rate doesn't change the WP lifetime from 20,000 years. As the fast corrosion rates increase, the fast corrosion time periods have a greater effect. The fast corrosion rates would have to be at a rate of  $10^{-3}$  cm/year for 1.19 year to decrease the WP lifetime to less than 10,000 years. Similar WP lifetimes less than 10,000 years would be obtained at a rate of  $10^{-2}$  cm/year for 0.119 years. The condition of  $10^{-2}$  cm/year or 1.19 years is unrealistically aggressive, considering (i) the transient curve of Figure (4), (ii) analyses presented in Peer Review of the Waste Package Material Performance <sup>[15]</sup>, and (iii) usual active corrosion rates discussed previously. Quantitative justifications of the perturbation are not available now with respect to the current transient with sulfur segregation at various corrosion potentials.

## CONCLUSIONS

- (1) The high temperature (above 100° C) deliquescence relative humidity from mixed salt deposits on the waste package (WP) was simulated by changing the critical relative humidity ( $RH_{critical}$ ) for aqueous corrosion from (60–65) pct to (35–60) pct.
- (2) For the base case values of the critical potential for localized corrosion, the estimated dose increased from 0.05 to 1 mrem/year in 10,000 years when the  $RH_{critical}$  was altered.
- (3) For modified values of the critical potential for localized corrosion the estimated dose increased to 3.8 mrem/year at 10,000 years even without lowering  $RH_{critical}$ .
- (4) The inhibiting effects of nitrate was simulated by using a constant value for the repassivation potential. With the addition of nitrate the estimated dose decreased to 0.03 mrem/year at 10,000 years.
- (5) The beneficial effect of partial protection of the waste package was simulated by altering the value of the Cladding Protection Factor. Giving credit to the remaining surface area of the container (of the WP) after failure by localized corrosion reduces the rate of radionuclide release and the maximum estimated dose decreased from 4 mrem/year with no credit to 0.4 mrem/year.

(6) To complement results from the sensitivity studies using TPA, a separate mathematical model was developed to assess enhanced uniform corrosion as a result of sulphur segregation at the interface of metal and passive film and subsequent spalling of passive film. The cyclic process of fast active (or non-passive) corrosion followed by slow passive corrosion could result in the WP lifetime less than 10,000 years at fast corrosion rate,  $10^{-2}$  cm/year, or the transient time, 1.19 years. However,  $10^{-2}$  cm/year or 1.19 years is an unrealistically aggressive condition.

This study suggests that with the sufficient amount of inhibitors or by giving credit to remaining WP surface area exposed from localized corrosion or stress corrosion cracking, the estimated dose is less than 0.4 mrem/year. Anodic sulfur segregation is unlikely to reduce significantly the WP lifetime.

Disclaimer: The NRC staff views expressed herein are preliminary and do not constitute a final judgment or determination of the matters addressed or of the acceptability of a license application for a geologic repository at Yucca Mountain. This presentation is also an independent product of the Center for Nuclear Regulatory Analyses and does not necessarily reflect the view or regulatory position of the NRC.

## REFERENCES

1. S. Mohanty, T. J. McCartin, and D. W. Esh, Total-system Performance Assessment Code (TPA), Version 4.0 Code: Module Description and User's Guide, Center for Nuclear Waste Regulatory Analyses, San Antonio, Texas, 2002
2. Bechtel SAIC Company, LLC, Technical Basis Document No. 5: In-Drift Chemical Environment, Rev.1, 2003
3. U.S. Nuclear Regulatory Commission, Integrated Issue Resolution Status Report, NUREG-1762, Washington, D.C., 2002
4. R. Jones, Metallurgical Stability and Radiation Effects, Peer Panel on Waste Package Performance, presented to U.S. Department of Energy and Bechtel SAIC, 2002
5. R. T. Pabalan, L. Yang, and L. Browning, Effects of Salt Formation on the Chemical Environment of Drip Shields and Waste Packages at the Proposed Nuclear Waste Repository at Yucca Mountain, Nevada, CNWRA 2002-03, Center for Nuclear Waste Regulatory Analyses, San Antonio, Texas, 2002
6. Electric Power Research Institute (EPRI), Evaluation of the Proposed High-Level Radioactive Waste Repository at Yucca Mountain Using Total System Performance Assessment, Phase 6, Palo, Alto, CA, 2002
7. C. Brossia, L. Browning, D. Dunn, O. Moghissi, O. Pensado, and L. Yang, Effect of Environment on the Corrosion of Waste Package and Drip Shield Materials, CNWRA 2001-03, Center for Nuclear Waste Regulatory Analyses, San Antonio, Texas, 2001
8. T. Ahn, *Waste Management*, 1994, Vol. 14, pp. 393 - 408
9. D. Esh, Performance Assessment Perspective on the Behavior of Engineered Barrier, presented to Advisory Committee on Nuclear Waste, U.S. Nuclear Regulatory Commission, 2003
10. Z. Szklarska-Smialowska, *Pitting Corrosion of Metals*, National Association of Corrosion

Engineers, Houston, Texas, 1986, p. 179 and p. 237,

11. P. Marcus, "Sulfur-Assisted Corrosion Mechanisms and the Role of Alloyed Elements."

*Corrosion Mechanisms in Theory and Practice*. P. Marcus and I. Olefjord, eds. New York City, New York, Marcel Dekker, 1995. p. 239

12. O. Pensado, D. S. Dunn, G. A. Cragolino, and V. Jain, Passive Dissolution of Container Materials - Modeling and Experiments, CNWRA 2003-01, Center for Nuclear Waste Regulatory Analyses, San Antonio, Texas, 2003

13. D. W. Shoesmith, S. Sunder, B. M. Ikeda and F. King, The Development of a Mechanistic Basis for Modeling Fuel Dissolution and Container Failures under Waste Vault Conditions, Mat. Res. Soc. Symp. Proc., 1989, Vol. 127, pp. 279 - 291

14. H. Jain, T. Ahn, and P. Soo, A Technique for Characterizing Crevice Corrosion under Hydrothermal Conditions, American Society for Testing and Materials, Special Technical Testing Publication 866, 1985

15. U.S. Department of Energy, Waste Package Materials Performance Peer Review Panel, Final Report, February 28, 2002